Journal of Geodynamics 54 (2012) 13–20

Contents lists available at SciVerse ScienceDirect

Journal of Geodynamics

journal homepage: http://www.elsevier.com/locate/jog

Stress field around the Coloumbo magma chamber, southern Aegean: Its significance for assessing volcanic and seismic hazard in Santorini

K.I. Konstantinou*, Te-Yang Yeh

Institute of Geophysics, National Central University, Jhongli 320, Taiwan

ARTICLE INFO

Article history:
Received 27 May 2011
Received in revised form 5 September 2011
Accepted 18 September 2011
Available online xxx

Keywords:
Coloumbo
Santorini
Aegean
Magma chamber
Stress
Hazard

ABSTRACT

Coloumbo submarine volcano lies 6.5 km offshore the NE part of the Santorini island complex and exhibits high seismicity along with vigorous hydrothermal activity. This study models the local stress field around Coloumbo's magma chamber and investigates its influence on intrusion emplacement and geometry. The two components of the stress field, hoop and radial stress, are calculated using analytical formulas that take into account the depth and radius of the magma chamber as these are determined from seismological and other observations. These calculations indicate that hoop stress at the chamber walls is maximum at an angle of 74° thus favouring flank intrusions, while the radial stress switches from tensile to compressive at a critical distance of 5.7 km from the center of the magma chamber. Such estimates agree well with neotectonic and seismological observations that describe the local/regional stress field in the area. We analyse in detail the case where a flank intrusion reaches the surface very near the NE coast of Thera as this is the worst-case eruption scenario. The geometrical features of such a feeder dyke point to an average volumetric flow rate of 9.93 $m^3 s^{-1}$ which corresponds to a Volcanic Explosivity Index of 3 if a future eruption lasts about 70 days. Hazards associated with such an eruption include ashfall, ballistic ejecta and base surges due to explosive mixing of magma with seawater. Previous studies have shown that areas near erupting vents are also foci of moderate to large earthquakes that precede or accompany an eruption. Our calculations show that a shallow event (3–5 km) of moment magnitude 5.9 near the eruptive vent may cause Peak Ground Acceleration in the range 122–177 $cm\,s^{-2}$ at different locations around Santorini. These values indicate that seismic hazard even due to a moderate earthquake near Coloumbo, is not trivial and may have a significant impact especially on older buildings at Thera island.

1. Introduction

The Santorini island complex consists of five islands (Thera, Therasia, Palea and Nea Kameni, Aspronisi) that delineate a flooded caldera formed after several cycles of explosive volcanic activity over the last 400 ka (Bond and Sparks, 1976; Heiken and McCoy, 1984; Druitt and Francaviglia, 1992; Vougioukalakis and Fytikas, 2005) (Fig. 1). The last of these cycles started with the Late Bronze Age (LBA) eruption (ca. 1628 BC) which involved phreatomagmatic explosions and extended pyroclastic flows that destroyed some early human settlements near Akrotiri. The LBA event probably also triggered a tsunami that was thought to have affected the whole of the Eastern Mediterranean (Dominey-Howes, 2004 and references therein). Subsequently, many authors have contested this view mostly based on the lack of such tsunami deposits outside the southern Aegean (Dominey-Howes, 2004) and on numerical simulations (Pareschi et al., 2006). Activity after the LBA eruption continued in a diminishing trend with several smaller eruptions, the last one having occurred in the early 1950s. The small islands of Palea and Nea Kameni were created by this post-eruptive activity and presently exhibit only low-temperature (~17 °C) hydrothermal fluid venting (Sigurdsson et al., 2006).

At a distance of about 6.5 km from the NE coast of Thera island lies Coloumbo volcano, expressed by a submarine crater of 1.5 km diameter and maximum crater floor depth of 500 m. Submarine observations have revealed that the area of the Coloumbo crater exhibits vigorous hydrothermal activity manifested by high-temperature (~220 °C) gas emission plumes rising from numerous vents (Sigurdsson et al., 2006). Deployment of temporary seismic networks has revealed that the area around Coloumbo exhibits much higher seismicity than that inside the Santorini caldera (Bohnhoff et al., 2006; Dimitriadis et al., 2009). This seismicity consists mainly of microearthquakes ($M_L < 4$) that form various clusters around the Coloumbo crater at depths between 2 and 20 km. Earthquake activity is also persistent to the NE of Coloumbo delineating a tectonic zone that in 1956 generated the large (M_w 7.6) Amorgos earthquake and subsequent tsunami (Konstantinou, 2010 and references therein). The last eruption of Coloumbo occurred in 1650

* Corresponding author. Fax: +886 3 4222044.
E-mail address: kkonst@ncu.edu.tw (K.I. Konstantinou).

0264-3707/$ – see front matter © 2011 Elsevier Ltd. All rights reserved.
doi:10.1016/j.jog.2011.09.003

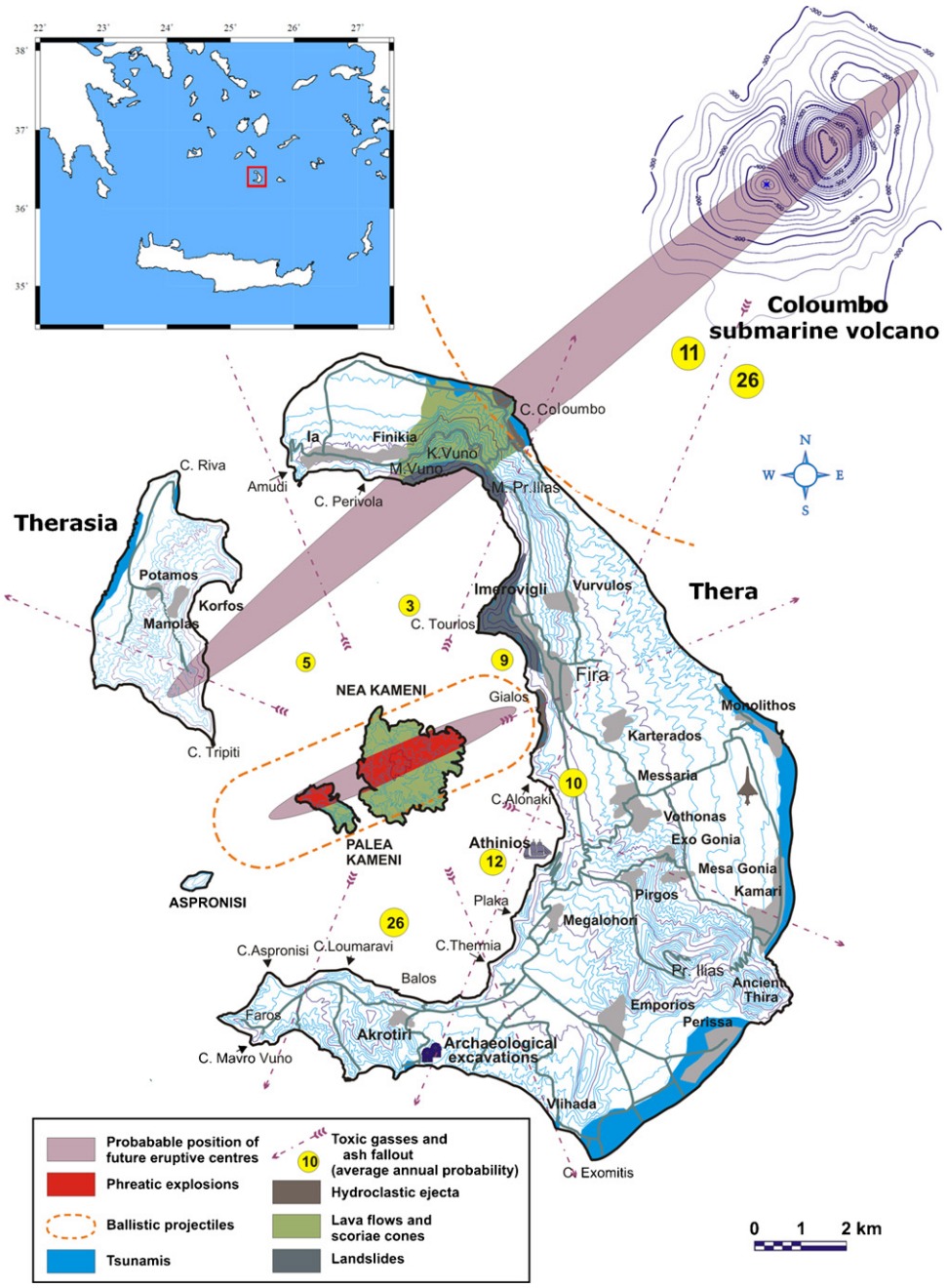

Fig. 1. Map of the Santorini island complex also depicting the volcanic hazards zonation due to a future eruption within the caldera or at Coloumbo (map compiled by G. Vougioukalakis also available from http://ismosav.santorini.net). Contours show the bathymetry in meters around the Coloumbo crater. The inset at the upper left-hand side shows the position of the island complex in the southern Aegean with a red square. (For interpretation of the references to colour in this figure legend, the reader is referred to the web version of the article.)

AD and involved the formation of pumice rafts as well as subaerial tephra fallout while eruptive activity was preceded/accompanied by strong earthquakes (Dominey-Howes et al., 2000). Historical accounts also mention that this eruption generated a large tsunami that inundated the eastern coast of Thera to a distance of 2 miles, depositing large submarine boulders and sediments (see Dominey-Howes et al., 2000 and references therein). Table 1 summarizes the volcanological characteristics of this eruption as listed in the Global Volcanism database of the Smithsonian Institution.

The Greek Institute of Geological and Mineral Exploration (IGME) has compiled a map of volcanic hazard zones for Santorini based mostly on information taken from historical sources about past eruptive activity (Fig. 1). This map identifies five different potential hazards and their corresponding zonation: (a) phreatic explosions, (b) ballistic projectiles, (c) tsunamis, (d) toxic gas/ashfall, and (e) landslides. As far as Coloumbo is concerned, the map delineates a zone of probable eruptive centers that extends from the Coloumbo crater up to Therasia. It also considers possible that ballistic projectiles from Coloumbo may affect the NE coast of Thera, while toxic gases and ashfall are expected to affect the whole of the Santorini area. In this work, we aim at improving the understanding of hazards stemming from future eruptive activity of Coloumbo by considering the stress field around its magma chamber and how this affects intrusion emplacement and geometry. First we give an overview of the available information about the Coloumbo magma chamber derived from seismological and

Table 1
Summary of the available information about the 1650 AD eruption of Coloumbo submarine volcano taken from the Global Volcanism Database of the Smithsonian Institution (http://www.volcano.si.edu).

Start date	1650 September 27
Stop date	1650 December 7
VEI	4?
Tephra volume	$>5.5 \pm 5.0 \times 10^8$ m^3
Type of eruption	flank/explosive

geochemical observations. We then use analytical models for the calculation of the hoop and radial stress components which have a direct effect on magma emplacement. These estimates are also correlated with other seismological, geological and neotectonic observations for the purpose of further constraining our results. Finally, we discuss how these first-order estimates have an impact not only on volcanic but also seismic hazard assessment for Santorini, since a future eruption will likely be accompanied by intense seismic activity.

2. The Coloumbo magma chamber

In a recent study, Dimitriadis et al. (2010) used local earthquake tomography in order to obtain P- and S-wave velocity images of the Coloumbo magma chamber. The authors used a dataset consisting of 137 local earthquakes with 1600 P-phases and 1521 S-phases recorded at 25 seismic stations. Most of the stations were operating on the Santorini island complex and some others on the nearby islands (Ios, Amorgos, Anafi) offering an improved azimuthal coverage. Despite this, the tomographic inversion faced problems due to ray coverage inhomogeneity produced by the fact that most earthquakes occurred around Coloumbo and were recorded by stations on Santorini. A corollary of this problem is the vertical smearing of the resulting tomographic images which needs to be taken into account when interpreting them. However, Dimitriadis et al. (2010) point out that smearing also depends on the direction of the tomographic cross-section, with a NW–SE direction exhibiting less pronounced effects.

Fig. 2 shows two of these tomographic cross-sections corresponding to P- and S-wave velocity structure respectively. In both of these images there is a well-defined region of negative velocity perturbation (up to −5%) that may represent low velocity material such as magma and/or crystal mush. The shape of the anomaly is approximately circular with a radius of 1.5–1.6 km while the depth of its center varies in the two images (5.5 km for P-wave and 6.8 km for S-wave structure). Considering this uncertainty it would be helpful to utilize additional observations for the purpose of constraining the depth of the proposed magma chamber. Cantner et al. (2010) have determined preliminary estimates of pre-eruption volatile contents from lava samples discharged during the 1650 AD eruption. Their results indicate an average value of 6.0 wt.% which corresponds to a pre-eruption storage pressure of 180 MPa. Assuming a density of 2640 kg m^{-3} for the surrounding rocks (upper crust can be represented by quartzite see Konstantinou, 2010) and a magma chamber depth of 6.8 km we obtain a lithostatic pressure of 176 MPa. Taking into account the pressure exerted by the overlying water column and assuming a mean water depth of 250 m around Coloumbo, we obtain a hydrostatic pressure of 2.5 MPa. In this way the total pressure in the magma chamber is 178.5 MPa which is very close to the value reported by Cantner et al. (2010). Therefore it seems that the depth derived by the S-wave tomographic image is more consistent with the geochemical results.

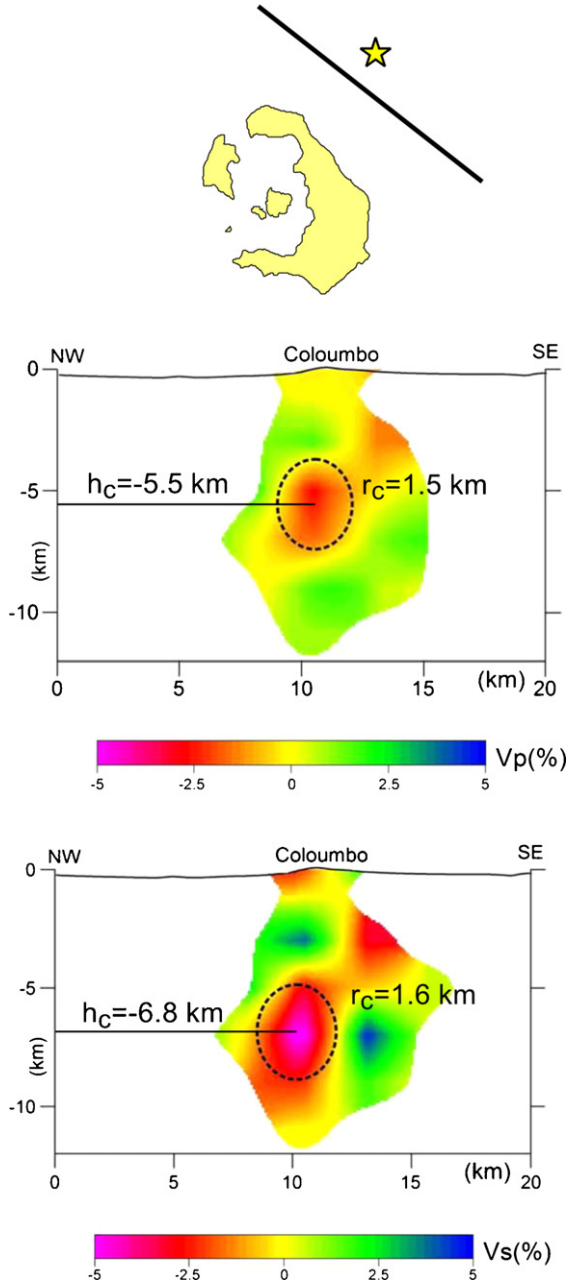

Fig. 2. P- and S-wave tomographic images beneath Coloumbo submarine volcano (after Dimitriadis et al., 2010). The orientation of the cross-sections relative to Santorini is shown on the top map. The colours correspond to percentage of velocity perturbation according to the scales shown at the bottom of each plot. The possible location of the Coloumbo magma chamber is delineated by a dashed line along with the depth h_c and radius r_c for both P- and S-wave images (see text for more details). (For interpretation of the references to colour in this figure legend, the reader is referred to the web version of the article.)

3. Hoop and radial stress

A magma chamber can be considered as a two-dimensional circular cavity surrounded by an isotropic and homogeneous medium (Fig. 3). This cavity may generate a stress field pattern depending on the imposed loading conditions. Obviously, the consideration of only two dimensions and the assumption of isotropy and homogeneity are simplifications of the real conditions around magma chambers. However, as Gudmundsson (2006) has shown, this simplified representation can yield credible results that are of great importance when assessing volcano hazards. Here we also show

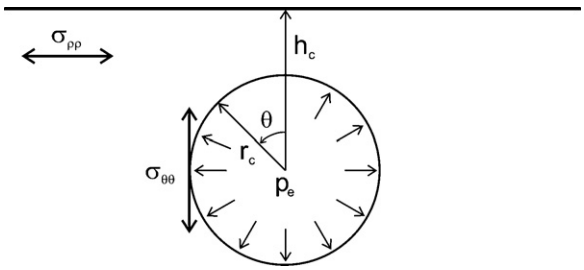

Fig. 3. Model of a circular cavity representing the magma chamber at depth h_c, radius r_c subject to overpressure p_e that is embedded in an elastic half-space. The stress field generated by this loading condition consists of the hoop stress ($\sigma_{\theta\theta}$) and radial stress ($\sigma_{\rho\rho}$). The hoop stress varies as a function of the angle θ.

that the results obtained from such an approach are consistent to first-order with tectonic and seismological observations around Coloumbo.

McTigue (1987) obtained analytical expressions for the stress around such a cavity by using the method of reflections and considering solutions of the form of perturbation expansions in powers of the ratio r_c/h_c. The author assumed that the magma chamber is subject to excess magmatic pressure p_e and lies inside an elastic half-space. The two components of this stress field are the hoop stress around the wall of the chamber indicated as $\sigma_{\theta\theta}$ and the radial stress away from the chamber that is symbolized as $\sigma_{\rho\rho}$. For the hoop stress the expression is given by

$$\sigma_{\theta\theta} = \frac{1}{2} + \epsilon^3(\alpha_0 + \alpha_2\cos^2\theta) + \epsilon^4(\beta_1\cos\theta + \beta_3\cos^3\theta) + \epsilon^5(\gamma_0 + \gamma_2\cos^2\theta + \gamma_4\cos^4\theta) \quad (1)$$

where the coefficients $\alpha_0, \alpha_2, \beta_1, \beta_3, \gamma_0, \gamma_2, \gamma_4$ are functions of the Poisson ratio ν (see Eq. 54 of McTigue, 1987), ϵ is the ratio r_c/h_c and θ is the angle defined in Fig. 3. The hoop stress estimated from this expression is dimensionless and scaled according to the assumed overpressure p_e inside the magma chamber. The corresponding expression for the radial stress is

$$\sigma_{\rho\rho} = 2\epsilon^3\left[\frac{2-\nu}{(\rho^2+1)^{3/2}} - \frac{3}{(\rho^2+1)^{5/2}}\right] \quad (2)$$

where ρ is the dimensionless distance from the center of the magma chamber scaled according to the depth h_c of the magma chamber. We use these expressions in order to evaluate the hoop and radial stress around the Coloumbo magma chamber taking $\epsilon = 0.23$ ($r_c = 1.6$ km, $h_c = 6.8$ km) and $\nu = 0.25$ which is consistent with the ratio of P- over S-wave velocity of 1.74 found in Santorini (Zhu et al., 2006). Fig. 4 shows the results of this evaluation for the two stress field components, $\sigma_{\theta\theta}$ as a function of the angle θ and $\sigma_{\rho\rho}$ as a function of the dimensionless distance ρ.

The hoop stress exhibits a maximum value at an angle $\theta = 74^\circ$ which indicates the location in the magma chamber wall that may rupture during dyke emplacement. This result implies that dyke intrusions may initiate at the flanks of Coloumbo magma chamber rather than near its top. Such a situation is expected at volcanoes that do not possess a large edifice that would otherwise focus tensile stresses near its summit (Pinel and Jaupart, 2003). Part of the edifice at Coloumbo was destroyed either after the 1650 AD eruption or much earlier, therefore only its SW part with a radius of about 1.6 km is preserved. The imaged magma chamber is not located directly beneath the remaining edifice, hence it is doubtful whether its loading has any significant effect on the rupture location.

On the other hand, the radial stress varies from tensile (negative) at small distances, to compressive (positive) at larger distances. The

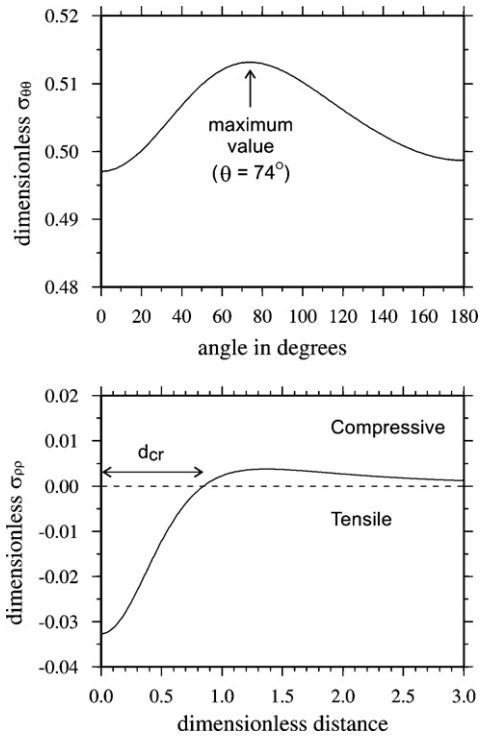

Fig. 4. Diagrams showing the variation of hoop and radial stress for the Coloumbo magma chamber. Top panel: Hoop stress as a function of the angle θ where a maximum exists at 74°; Lower panel: radial stress as a function of dimensionless distance where at critical distance d_{cr} the stress switches from tensile to compressive (see text for more details).

critical distance d_{cr} where this change occurs is equal to $\rho = 0.84$ which corresponds to 5.7 km (0.84×6.8 km) from the center of the magma chamber (Fig. 5). The area delineated by this distance indeed exhibits tensile local stresses as demonstrated by Dimitriadis et al. (2009) using a set of well-constrained earthquake focal mechanisms. Most of the fault plane solutions exhibit normal

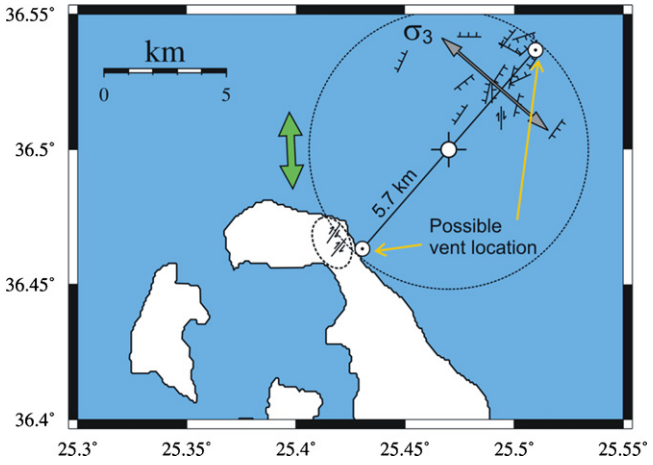

Fig. 5. Map showing the modeling results of the magma chamber stress field combined with available seismological and neotectonic observations. The large circle indicates the extent of the tensile radial stress having as its center the Coloumbo magma chamber if the depth of the magma chamber is taken as 6.8 km. The local σ_3 principal axis orientation is taken from the stress tensor derived by Dimitriadis et al. (2009). Hatched line segments represent orientations of seismic faults identified by the stress tensor inversion method. Neotectonic observations of two strike-slip faults near Cape Coloumbo are also highlighted with an ellipse. The green double arrow represents principal axes of the regional strain tensor for this area determined from GPS data (from Hollenstein et al., 2008).

faulting and their inversion for the purpose of deriving the orientation of the principal stress axes shows that σ_3 is orientated along the NW–SE direction (strike ~311°) and is subhorizontal (dip ~18°). Using a shallower depth for the magma chamber (e.g. 5.5 km so $0.84 \times 5.5 = 4.6$ km) would have the effect of underestimating the extent of the tensile area around it. This confirms that our initial depth estimate is also consistent with seismological observations. Superimposed to this local stress field is the regional one that affects the whole of the Aegean area and according to GPS measurements it exhibits N–S extension (Hollenstein et al., 2008). The result of this superposition should be an area that experiences strike-slip motion and clockwise rotation. Neotectonic observations show such an area in the NE part of Thera island where this kind of faulting occurs at the border of the tensile region (Dimitriadis et al., 2009).

4. Intrusion emplacement and volumetric flow rate

It is now interesting to investigate how such a stress pattern would influence the emplacement of magma injected from the Coloumbo magma chamber, since this has direct implications for volcanic hazard. The first step towards magma injection is the rupture of the magma chamber walls, therefore the maximum hoop stress should exceed the tensile strength of the surrounding rocks. For a typical crystalline host rock the tensile strength is in the range of 0.5–6 MPa (e.g., Amadei and Stephansson, 1997). The maximum hoop stress calculated previously has to be multiplied by an assumed overpressure in order to be converted to physical units. By assuming an overpressure equal to 12 MPa we obtain $\sigma_{\theta\theta} = 6.2$ MPa which exceeds the maximum tensile strength of most host rocks. At this point it should be mentioned that for most chambers the main stress concentration would be at local irregularities in their walls, in which case the overpressure needed for rupture can be equal to the tensile strength of the rock rather than twice this value assumed here. The newly formed fracture may then propagate away from the magma chamber and this propagation is controlled by the static magmatic overpressure Δp inside the crack (e.g. Gudmundsson et al., 1999)

$$\Delta p = p_e + (\rho_r - \rho_m)gh + \Delta\sigma \tag{3}$$

where p_e is magma overpressure above the lithostatic one, g is acceleration of gravity, h is depth, ρ_r is density of the rock, ρ_m is density of magma and $\Delta\sigma$ is the difference between vertical (σ_v) and horizontal (σ_h) compressive stress. While p_e decays progressively due to viscous drag effects and the density difference becomes zero or even negative at shallow depths, the term $\Delta\sigma$ effectively controls the propagation. The condition for propagation is that $\Delta\sigma = \sigma_v - \sigma_h$ remains positive and this can happen if the horizontal stress σ_h is equal to the least compressive stress σ_3. The exact path that this intrusion will take is controlled by the mechanical properties of the rocks surrounding the magma chamber, especially if these consist of alternating layers of soft pyroclastic material and stiff lava flows as found in many volcanoes. In fact, numerical models simulating these conditions predict that a spherical magma chamber, subject to excess magmatic pressure as the only loading condition, tends to favour inclined sheets (Gudmundsson, 2006 and references therein). This situation seems to be occuring around Coloumbo since the tomographic images (Fig. 6 inset) indicate a low-velocity zone emanating from the magma chamber along a SW direction. Above this zone there are almost horizontal high velocity bodies with positive velocity perturbations between 5 and 10%. These may represent series of layers of pyroclastic rocks and lavas that have accumulated from previous eruptions. Intrusions probably start as inclined sheets near the magma chamber later becoming subvertical dykes further away from it. Observations at several exhumed volcanoes show that most of these intrusions are

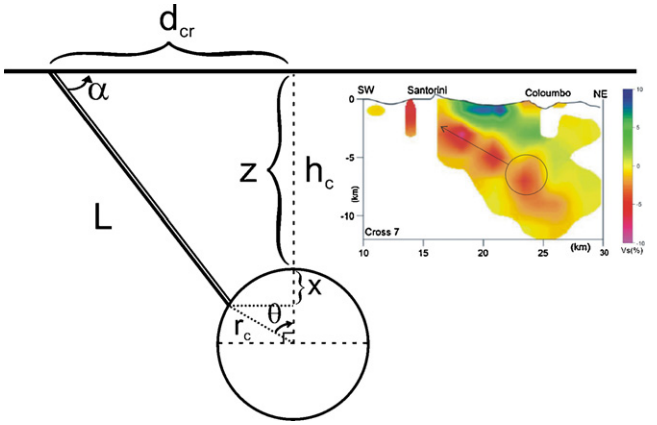

Fig. 6. Cartoon showing the possible geometrical configuration of a dyke injected from the Coloumbo magma chamber. The dyke originates at the point of maximum hoop stress at a vertical distance x from the top of the magma chamber which lies at depth z from the surface. The intrusion has a down-dip length L and forms an angle α with the Earth surface at a distance d_{cr} from the magma chamber. Other symbols are the same as in Fig. 3. The inset shows a NE–SW cross-section of the tomographic model of Dimitriadis et al. (2010) where a low-velocity linear feature can be seen emanating from the Coloumbo magma chamber. It should be noted that due to vertical smearing it is not possible to infer the exact shape and thickness of this low-velocity anomaly.

arrested at various depths without being able to feed an eruption (Gudmundsson, 2002). Tomographic results seem to support this view, since they show that part of the low-velocity zone extending from Coloumbo, terminates beneath the Santorini caldera before it can reach the Earth's surface.

We focus on the possibility that during a future eruption magma will follow the pathway marked by this low-velocity zone and place the eruptive vent location perpendicular to the direction of σ_3. In this case we attempt to calculate the apparent dip of the inclined sheet along the NE–SW direction in an effort to calculate the magma flow rate which is important in terms of having an estimate of the volume of erupted material. Fig. 6 shows the geometrical configuration we assume in order to find the angle α

$$\tan\alpha = \frac{z+x}{d_{cr} - r_c\sin\theta} = \frac{h_c - r_c + r_c(1-\cos\theta)}{d_{cr} - r_c\sin\theta} \tag{4}$$

It is then possible to estimate the down-dip length L of the sheet by using the trigonometric relationship

$$L = \frac{z+x}{\sin\alpha} = \frac{h_c - r_c + r_c(1-\cos\theta)}{\sin\alpha} \tag{5}$$

By substituting the corresponding values to these equations we obtain an angle $\alpha = 56°$ and a length $L = 7.7$ km. Observations of exposed feeder dykes in Miyakejima volcano, Japan, reveal that their aperture u is of the order of 1 m even though this may increase when the intrusion reaches very near the Earth's surface (Geshi et al., 2010). The surface width W can also be estimated through the aspect ratio (W/u) which usually takes values of around 1000 (see Gudmundsson, 2002). This means that for an aperture of 1 m the width should be 1000 m. Having estimates of these geometrical characteristics we can now calculate the volumetric flow rate of magma given by (Gudmundsson and Brenner, 2005)

$$Q = \frac{u^3 W}{12n}\left[(\rho_r - \rho_m)g\sin\alpha - \frac{\partial p_e}{\partial L}\right] \tag{6}$$

where n is magma viscosity and $\partial p_e/\partial L$ is the pressure gradient. We use a value of $10^{4.2}$ Pa s for the viscosity (Hellwig, 2006), which is consistent with rhyolitic magma at a temperature of 800 °C rich in volatiles like the magma erupted during the 1650 AD eruption (Cantner et al., 2010). Then for a pressure gradient of -1558 Pa m^{-1}

(p_e = 12 MPa, L = 7700 m) we calculate that the flow rate of magma through the sheet is about 9.93 $m^3\ s^{-1}$. This may be an average estimate, since it is expected that flow rates during the early stages of an eruption may be much higher than this value due to wider aperture and larger initial overpressure. If a future eruption lasts the same period of time as the 1650 AD eruption (~70 days), the flow rate we calculated indicates that $6 \times 10^7\ m^3$ of material would be erupted. This quantity implies an eruption size consistent with Volcanic Explosivity Index (VEI) of 3.

5. Future eruption and associated hazards

A global survey of submarine eruptions has shown that volcanic activity is likely to become subaerial only if the water depth near the vent is less than 100 m (Mastin and Witter, 2000). Therefore the position where a dyke injected from the Coloumbo magma chamber, may reach the Earth's surface is of paramount importance for volcanic hazard assessment. In our analysis we focused on the case where the dyke breaks through very near the island of Thera. This is clearly the most dangerous scenario, as the eruptive vent will lie on the seafloor perhaps some hundreds of meters from the coast and at a depth between 50 and 100 m based on the bathymetric map published by Perissoratis (1995). On the other hand, if the dyke propagates to the NE direction towards the open sea (where depths are considerably larger than 100 m) a subaerial eruption can be considered less probable. Tomographic results suggest however, that future intrusions are more likely to occur along the SE direction where a magma pathway is already established.

The hazards associated with a subaerial eruption from a shallow vent near the coast of Thera mainly involve ashfall (and probable toxic gas release), ballistic projectiles and base surges. The first of these hazards is expected to affect the whole of the island complex and depends on weather conditions at the time of the eruption, therefore it is difficult to predict its impact. On the other hand, the hazard from ballistic projectiles is far more predictable and calculations show that spherical blocks of 40 cm diameter, subject to variable air drag and initial velocities in excess of 150 $m\ s^{-1}$, may reach a distance of up to 2.5 km from the vent (Mastin, 2001). This means that a larger area in NE Thera is vulnerable to such ejecta than what was previously assessed (Fig. 7). Base surges are generated by large discrete explosions produced by the mixing of erupted magma with seawater. They form ring-shaped clouds of water and debris that propagate at high velocity along the ground or water surface. Usually their radius is within the range of 0.5–2.5 km, however, it can reach a value of 6 km if the explosions occur in shallow water and the magma-water mixture attains a ratio 3–5.5:1 (Mastin, 1995). A base surge of this extent is a rare phenomenon, but was nevertheless observed during the 1965 eruption of Lake Taal volcano claiming the lives of several tens of people (Moore et al., 1967). It should be noted that the size of the eruption (as indicated by its VEI) is not proportional to the potential for a large base surge (see Mastin and Witter, 2000). Hence, a relatively small eruption (VEI 3–4) at Coloumbo may generate a catastrophic base surge should it occur near shallow water. Based on the experience from Lake Taal, it is possible that such a base surge would move with hurricane velocity following the surface topography, having temperatures up to 100 °C. Apart from human casualties, its consequences may be severe for buildings and infrastructure (e.g. power/communication lines) on Thera as both Fira and Ia may lie in its path (Fig. 7).

A tsunami may also follow a submarine eruption and as mentioned earlier there are several historical accounts about the occurrence of a catastrophic tsunami after the onset of the 1650 AD Coloumbo eruption. Dominey-Howes et al. (2000) studied the lithostratigraphy of three trench excavations close to the villages

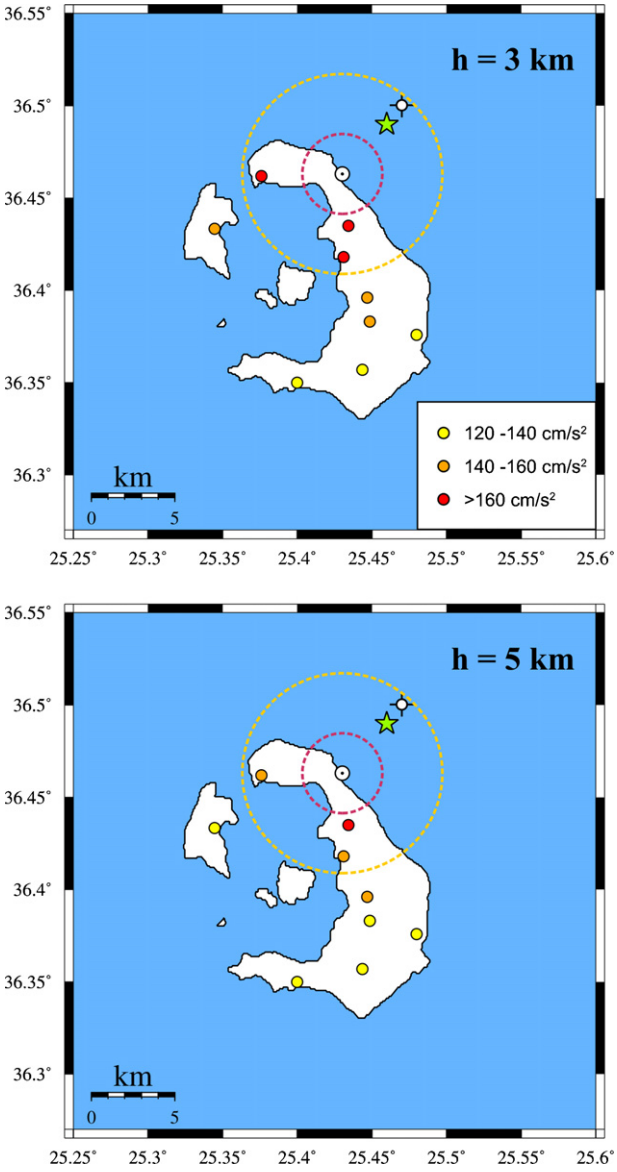

Fig. 7. Top panel: Map of the Santorini island complex showing possible zonation of ballistic ejecta (red circle with radius 2.5 km), base surge (yellow circle with radius 6 km) and PGA values due to a M_w = 5.9 shallow (3 km) earthquake accompanying the eruptive activity. The hypothesized eruptive vent is located south of Cape Coloumbo and the epicenter of the earthquake (green star) lies at a distance 4.7 km from it. The coloured dots represent calculated values of PGA at different locations (see text for more details) and follow the colour scale shown at the right. Lower panel: The same for an earthquake with hypocentral depth of 5 km. (For interpretation of the references to colour in this figure legend, the reader is referred to the web version of the article.)

of Kamari and Perissa which lie within the reported inundation zone of this tsunami. The authors found no evidence of tsunami related sediments and concluded that if such a tsunami did occur, it was fairly minor without leaving any sedimentary signature. This result agrees with the suggestion that volcanogenic tsunamis are smaller due to the smaller volume of water they displace compared to faulting or landslide generated tsunamis (Mastin and Witter, 2000). One could therefore argue that the tsunami hazard from a future eruption similar in volume to that of 1650 AD is probably low. Nevertheless, a proper analysis of tsunami hazard due to such activity can only be evaluated through numerical simulations considering a range of scenarios. The results presented in this study may be useful to tsunami modelers in this respect.

In a first of its kind study for Santorini, Dominey-Howes and Minos-Minopoulos (2004) conducted a survey of volcanic hazard and risk awareness over the local population and municipal officers. The survey revealed that most of the local residents did not know that Coloumbo volcano is active, while municipal officers confirmed that there is no evacuation plan in case of a volcanic eruption. Taking into account the large influx of tourists during the summer months and the worst-case eruption scenario that was analysed in this study, it is clear that the danger posed is very serious. Efforts should be directed towards educating the local population about volcanic hazards and designing an emergency plan in case of a future eruption that would also include evacuation procedures when this is deemed necessary.

6. Seismic hazard due to volcanic activity

Except from the volcanic hazards discussed previously, a future eruption originating from Coloumbo may also be preceded and/or accompanied by intense seismic activity. This activity can take the form of numerous small events but it can also be expressed through the occurrence of a larger event. Here we will examine the hazard stemming from the latter possibility. We note that a swarm of smaller events may also cause damage to built structures due to accumulation of hysteritic energy as shown by Festa et al. (2004). However, the investigation of this issue as well as the issue of seismic hazard in Santorini due to a large tectonic earthquake (like the 1956 Amorgos event) will be the topic of a future study.

Zobin (2001) compiled a catalogue of moderate and large earthquakes (M_w 4.6–7.1) that were related to volcanic activity during the 20th century. Analysis of this catalogue showed that the expected maximum magnitude depends on the type of eruption and that the recurrence time of such events is usually more than 100 years. The distance of these earthquakes from the erupting vent exhibits an anti-correlation with the crustal thickness in the area. These results indicate that for a submarine eruption like the one expected from Coloumbo, the maximum moment magnitude is 5.9, while its distance D in km from the hypothesised vent is given by

$$\log D = 3.67 - 2.14 \log H \tag{7}$$

where H is the crustal thickness which for most of the southern Aegean is 25 km (e.g., Sodoudi et al., 2006). This yields D equal to 4.7 km and accordingly we place the epicenter at such a distance to the NE of the vent (Fig. 7). For the purpose of evaluating the seismic hazard posed to Santorini because of such an event we calculate intensities at several sites, including Fira and Ia. We use an intensity-distance law appropriate for volcanic areas derived by Zobin (2001) that predicts stronger attenuation of intensities and is likely to be more representative of the local conditions around Santorini. This law is given by the relationship

$$I = 0.66M_w - 1.13 \log R - 0.0072R + 3.73 \tag{8}$$

where I is intensity according to the Modified Mercalli scale, M_w is moment magnitude and $R = (\Delta^2 + h^2)^{1/2}$ with Δ being the epicentral distance and h the hypocentral depth. Intensities are then converted to Peak Ground Acceleration (PGA) a using the relationship derived by Koliopoulos et al. (1998) for the Greek region

$$\log a = 0.33I + 0.07. \tag{9}$$

We investigate two possible hypocentral depths at 3 and 5 km respectively and the results of these calculations are shown in Fig. 7. It can be seen that the shallower source also causes higher PGA values, the largest of them registered at the small village of Vurvulos (177 cm s^{-2}). Fira and Ia also register large values between 162 and 164 cm s^{-2} while the southern part of Thera and Therasia register smaller values (122–148 cm s^{-2}). Post-seismic field surveys in Greece indicate that damage to buildings occurs when PGA values exceed 110 cm s^{-2} (Papazachos and Papazachou, 1997). The new building code that came into force in 2000, assumes 160 cm s^{-2} as the maximum expected PGA value for Santorini. This should theoretically be adequate for the shaking caused by a near-field source as the one discussed here. However, buildings built before the year 2000, that are also the majority, have been constructed following lower standards regarding their ability to withstand strong shaking. Site effects due to the soft pyroclastic material that most buildings are founded on, is an extra complicating factor that has not been investigated to date. Secondary effects of strong ground motion are rockfalls or even landslides that may originate at unstable parts of the caldera rim at Thera. This is particularly true for Athinios port where rockfalls occur even without any external forcing (Antoniou and Lekkas, 2010). We can conclude therefore that seismic hazard related to volcanic activity at Coloumbo, even due to a moderate earthquake, is significant for the largest part of Thera.

7. Conclusions

The main conclusions of this study can be summarized as follows:

- The depth of the magma chamber beneath Coloumbo submarine volcano is constrained by seismological and geochemical observations to be 6.8 km which is also consistent with the analytical modeling of its stress field pattern. Hoop stress estimates as well as tomographic results point to the possibility of flank intrusions emanating from the magma chamber to the NE coast of Thera as the most likely pathway during a future eruption.
- The most dangerous scenario of a future eruption at Coloumbo is that the eruptive vent will be located very near Thera where the water depth is less than 100 m allowing the eruption to become subaerial. In this case, the NE part of the island which is also the most populated, will be vulnerable to ballistic projectiles and base surges as well as ashfall and toxic gas release. Previous studies have failed to detect sedimentological evidence of the tsunami that inundated the eastern coast of Thera during the 1650 AD eruption of Coloumbo. It is likely therefore that tsunami hazard from a future eruption is low, however, drawing firm conclusions requires extensive numerical simulations.
- An earthquake of moment magnitude 5.9 that would precede or accompany the eruption, may produce PGA values that will exceed 122 cm s^{-2} in the largest part of Thera and probably cause significant damage to older buildings along with secondary hazardous phenomena such as rockfalls or landslides. These empirically determined PGA estimates do not take into account local site effects due to the soft pyroclastic material that most buildings are founded on, therefore they may represent a lower bound.

Acknowledgements

We would like to thank the National Science Council of Taiwan for financial support in the form of a research grant awarded to the first author. This study forms part of Te-Yang Yeh's undergraduate research project. Agust Gudmundsson and Marco Bohnhoff provided helpful reviews that improved the original manuscript substantially.

References

Amadei, B., Stephansson, O., 1997. Rock Stress and Its Measurement. Chapman and Hall, London.

Antoniou, A.A., Lekkas, E., 2010. Rockfall susceptibility map for Athinios port, Santorini island, Greece. Geomorphology 118, 152–166, doi:10.1016/j.geomorph.2009.12.015.

Bohnhoff, M., Rische, M., Meier, T., Becker, D., Stavrakakis, G., Harjes, H.-P., 2006. Microseismic activity in the Hellenic Volcanic Arc, Greece, with emphasis on the seismotectonic setting of the Santorini-Amorgos zone. Tectonophysics 423, 17–33, doi:10.1016/j.tecto.2006.03.024.

Bond, A., Sparks, R.S.J., 1976. The Minoan eruption of Santorini, Greece. J. Geol. Soc. Lond. 132, 1–16.

Cantner, K., Carey, S., Sigurdsson, H., Vougioukalakis, G., Nomikou, P., Roman, C., Bell, K.L., Alexandri, M., 2010. Pre-eruption pressure, temperature and volatile content of rhyolite magma from the 1650 AD eruption of Koloumbo submarine volcano, Greece, V23B-2442. In: AGU Fall Meeting.

Dimitriadis, I., Karagianni, E., Panagiotopoulos, D., Papazachos, C., Hatzidimitriou, P., Bohnhoff, M., Rische, M., Meier, T., 2009. Seismicity and active tectonics at Coloumbo reef (Aegean sea, Greece): Monitoring an active volcano at Santorini volcanic center using a temporary seismic network. Tectonophysics 465, 136–149, doi:10.1016/j.tecto.2008.11.005.

Dimitriadis, I., Papazachos, C., Panagiotopoulos, D., Hatzidimitriou, P., Bohnhoff, M., Rische, M., Meier, T., 2010. P and S velocity structures of the Santorini-Coloumbo volcanic system (Aegean Sea, Greece) obtained by non-linear inversion of travel times and its tectonic implications. J. Volcanol. Geotherm. Res. 195, 13–30, doi:10.1016/j.jvolgeores.2010.05.013.

Dominey-Howes, D., 2004. A re-analysis of the Late Bronze Age eruption and tsunami of Santorini, Greece, and its implications for volcano-tsunami hazard. J. Volcanol. Geotherm. Res. 130, 107–132, doi:10.1016/S0377-0273(03)00284-1.

Dominey-Howes, D., Papadopoulos, G.A., Dawson, A.G., 2000. Geological and historical investigation of the 1650 Mt Coloumbo (Thera island) eruption and tsunami, Aegean Sea, Greece. Nat. Hazards 21, 83–96.

Dominey-Howes, D., Minos-Minopoulos, D., 2004. Perceptions of hazard and risk on Santorini. J. Volcanol. Geotherm. Res. 137, 285–310, doi:10.1016/j.jvolgeores.2004.06.002.

Druitt, T.H., Francaviglia, V., 1992. Caldera formation on Santorini and the physiography of the islands in the late bronze age. Bull. Volcanol. 54, 484–493.

Festa, G., Zollo, A., Manfredi, G., Polese, M., Cosenza, E., 2004. Simulation of earthquake ground motion and effects on engineering structures during the preeruptive phase of an active volcano. Bull. Seism. Soc. Am. 94, 2213–2221.

Geshi, N., Kusumoto, S., Gudmundsson, A., 2010. Geometric difference between non-feeder and feeder dykes. Geology 38, 195–198, doi:10.1130/G30350.1.

Gudmundsson, A., Marinoni, L.B., Marti, J., 1999. Injection and arrest of dykes: implications for volcanic hazards. J. Volcanol. Geotherm. Res. 88, 1–13.

Gudmundsson, A., Brenner, S.L., 2005. On the conditions of sheet intrusions and eruptions in stratovolcanoes. Bull. Volcanol. 67, 768–782, doi:10.1007/s00445-005-0433-7.

Gudmundsson, A., 2002. Emplacement and arrest of sheets and dykes in central volcanoes. J. Volcanol. Geotherm. Res. 116, 279–298.

Gudmundsson, A., 2006. How local stresses control magma-chamber ruptures, dyke injections, and eruptions in composite volcanoes. Earth Sci. Rev. 79, 1–31, doi:10.1016/j.earscirev.2006.06.006.

Heiken, G., McCoy, F., 1984. Caldera development during the Minoan eruption, Thira, Cyclades, Greece. J. Geophys. Res. 89, 8441–8462.

Hellwig, B.M., 2006. The viscosity of dacitic liquids measured at conditions relevant to explosive arc volcanism: determining the influence of temperature, silicate composition, and disolved volatile content, MS thesis, University of Missouri-Coloumbia.

Hollenstein, C., Müller, M.D., Geiger, A., Kahle, H.-G., 2008. Crustal motion and deformation in Greece from a decade of GPS measurements 1993–2003. Tectonophysics 449, 17–40, doi:10.1016/j.tecto.2007.12.006.

Koliopoulos, P.K., Margaris, B.N., Klimis, N.S., 1998. Duration and energy characteristics of Greek strong-motion records. J. Earth Eng. 2, 391–417.

Konstantinou, K.I., 2010. Crustal rheology of the Santorini-Amorgos zone: implications for the nucleation depth and rupture extent of the 9 July 1956 Amorgos earthquake, southern Aegean. J. Geodyn. 50, 400–409, doi:10.1016/j.jog.2010.05.002.

Mastin, L.G., 1995. Thermodynamics of gas and steam-blast explosions. Bull. Volcanol. 57, 85–98.

Mastin, L. G., 2001. A simple calculator of ballistic trajectories for blocks ejected during volcanic eruptions, US Geological Survey Open File Report, 01-45.

Mastin, L.G., Witter, J.B., 2000. The hazards of eruptions through lakes and seawater. J. Volcanol. Geotherm. Res. 97, 195–214.

McTigue, D.F., 1987. Elastic stress and deformation near a finite spherical magma body: resolution of the point source paradox. J. Geophys. Res. 92, 12931–12940.

Moore, J.G., Nakamura, K., Alcaraz, A., 1967. The 1965 eruption of Taal volcano. Science 151, 955–960.

Papazachos, B.C., Papazachou, K., 1997. The earthquakes of Greece, Ziti editions, Thessaloniki.

Pareschi, M.T., Favalli, M., Boschi, E., 2006. Impact of the Minoan tsunami of Santorini: simulated scenarios in the eastern Mediterranean. Geophys. Res. Lett. 33, L18607, doi:10.1029/2006GL027205.

Perissoratis, C., 1995. The Santorini volcanic complex and its relation to the stratigraphy and structure of the Aegean arc, Greece. Mar. Geol. 128, 37–58.

Pinel, V., Jaupart, C., 2003. Magma chamber behaviour beneath a volcanic edifice. J. Geophys. Res. 108, 2072, doi:10.1029/2002JB001751.

Sigurdsson, H., Carey, S., Alexandri, M., Vougioukalakis, G., Croff, K., Roman, C., Sakelariou, D., Anagnostou, C., Rousakis, G., Ioakim, C., Gogou, A., Ballas, D., Misaridis, T., Nomikou, P., 2006. Marine investigations of Greece's Santorini volcanic field. EOS 87, 337–342.

Sodoudi, F., Kind, R., Hatzfeld, D., Priestley, K., Hanka, W., Wylegalla, K., Stavrakakis, G., Vafidis, A., Harjes, H.-P., Bohnhoff, M., 2006. Lithospheric structure of the Aegean obtained from P and S receiver functions. J. Geophys. Res. 111, B12307, doi:10.1029/2005JB003932.

Vougioukalakis, G.E., Fytikas, M., 2005. Volcanic hazards in the Aegean area, relative risk evaluation, monitoring, and present state of the active volcanic centers, The south Aegean active volcanic arc: Present knowledge and future perspectives. Dev. Volcanol. 7, 161–183.

Zobin, V.M., 2001. Seismic hazard of volcanic activity. J. Volcanol. Geotherm. Res. 112, 1–14.

Zhu, L., Mitchell, B.J., Akyol, N., Cemen, I., Kekovali, K., 2006. Crustal thickness variations in the Aegean region and implications for the extension of continental crust. J. Geophys. Res. 111, B01301, doi:10.1029/2005JB003770.